2015

High-resolution model for noncontact atomic force microscopy with a flexible molecule on the tip apex

Chun-Sheng Guo
Key Laboratory of Advanced Technology of Materials (Ministry of Education), Superconductivity and New Energy R&D Center, Southwest Jiaotong University, Mail Stop 165#, Chengdu 610031, Sichuan, China

Michel Andre Van Hove
Hong Kong Baptist University, vanhove@hkbu.edu.hk

Xinguo Ren
Key Laboratory of Quantum Information, University of Science and Technology of China, Hefei 230026, Anhui, China

Yong Zhao
School of Materials Science and Engineering, University of New South Wales, Sydney, 2052 NSW, Australia

Citation

Guo, Chun-Sheng, Michel Andre Van Hove, Xinguo Ren, and Yong Zhao. "High-resolution model for noncontact atomic force microscopy with a flexible molecule on the tip apex." *Journal of Physical Chemistry C* 119.3 (2015): 1483-1488.

A high-resolution model for non-contact atomic force microscopy with a flexible molecule on the tip apex

Chun-Sheng Guo,[a,*] Michel A Van Hove,[b,] Xinguo Ren,[c,d,] Yong Zhao[a,e]

[a]*Key Laboratory of Advanced Technology of Materials (Ministry of Education), Superconductivity and New Energy R&D Center, Mail Stop 165#, Southwest Jiaotong University, Chengdu 610031, Sichuan, China*

[b]*Institute of Computational and Theoretical Studies and Department of Physics, Hong Kong Baptist University, Hong Kong, China*

[c]*Key Laboratory of Quantum Information, University of Science and Technology of China, Hefei 230026, Anhui, China*

[d]*Synergistic Innovation Center of Quantum Information & Quantum Physics,University of Science and Technology of China, Hefei, 230026, Anhui, China*

[e]*School of Materials Science and Engineering, University of New South Wales, Sydney, 2052 NSW, Australia*

*Corresponding Author: csguo@swjtu.edu.cn

Abstract

Experiments using non-contact atomic force microscopy (NC-AFM) with CO-molecule-functionalized tips have distinctly imaged chemical structures within conjugated molecules. Here we describe a detailed model based on an *ab initio* approach of the interaction force between the AFM tip and the sample molecule that yields atomic-scale images which agree very well with the experimental images we considered. The key ingredient of our model is to explicitly include the effect on the image due to the tilt of the CO molecule at the tip apex resulting from the lateral force exerted by the sample. Based on this model, we specifically discuss the distortion seen in AFM images. As reported very recently, the distortion in AFM images originates from an intrinsic effect, namely different extents of π-electron orbitals, as well as from an extrinsic effect, specifically CO tilt. We find that intrinsic distortion is scanning height dependent, attributing to the integrated electron density in the tip-sample overlapping region moving away from (the vertical projection of) the atom or bond positions. This intrinsic distortion is dominant in AFM images, although the atomic positions could be displaced even more by the extrinsic distortion due to CO tilt.

1. Introduction

In recent years non-contact atomic force microscopy (NC-AFM) with molecule-functionalized tips (MFT) operated in the frequency modulation mode[1] has reached unprecedented atomic resolution of molecules supported on solid substrates. Since the detailed imaging of the chemical structure of a pentacene molecule was accomplished in 2009,[2] the chemical structure of a variety of other conjugated molecules has also been imaged by NC-AFM.[3-12] Most impressively, the intricate chemical transformation of an individual molecule[6] as well as weak hydrogen-bonds between molecules were directly imaged.[8] In addition it was reported that it is possible to discriminate between bond orders of carbon-carbon bonds within polycyclic aromatic hydrocarbons and fullerenes.[5]

Despite the impressive success of the NC-AFM technique in resolving the chemical structure of individual molecules, the molecular geometry in the AFM image seems to be considerably distorted.[2,5,13-15] The chemical bonds are in general elongated and the lateral size of the molecule is enlarged. In certain cases, the apparent positions of atoms measured by AFM can be displaced by distances as large as 1 Å. This effect is much larger than the experimental uncertainty, or than possible geometry changes of the molecule due to its interaction with the substrate, which makes the accurate direct determination of a single molecule's geometry using the AFM technique a very challenging task. Under such circumstances, it is of crucial importance to understand the origin of this pronounced effect. It has been proposed[13-15] that the distortion of AFM images arises from the tilt of the CO molecule. However, with this assumption extremely small values for the lateral stiffness of tip are needed for a good artificial fitting.[15] Very recently, it was

suggested that distortion in AFM images originates from an intrinsic effect –different spatial extents of π-electron orbitals – and from an extrinsic effect –CO tilt.[16]

So far, direct comparison between experimental and simulated NC-AFM images has been rare. In previous studies based on *ab initio* calculations,[2,17] the lateral tip-sample interaction was ignored because it is very time consuming to relax the tip at every grid point within a 2-dimensional area. A molecule functionalizing the AFM tip is actually flexible at the apex and bent due to the lateral interaction during scanning, and the images obtained with rigid tips conceal many details and can be misleading. On the other hand, although the lateral tilt effect of CO tip has been considered in the simulation based on force field model, further analysis related to the electronic effect is difficult, and was even avoided altogether in one study.[18]

In this work, we firstly present a more accurate and detailed *ab initio* approach to simulate the AFM image; in particular, it includes specifically the effects of the tilt of the CO molecule under the influence of the sample as the tip is scanned across the sample such that it allows complete two-dimensional frequency shift maps to be calculated efficiently and compared directly to AFM experiments. Secondly, by comparing the simulated images which include or exclude the effect of the CO tilt with the electron density profiles between the CO tip and the sample, as well as with the chemical structures of the sample, the origin of the distortion of the AFM image can be studied in more detail.

2. Theoretical details

For convenience, we consider that the CO molecule which functionalizes the AFM tip, when far from the sample, is oriented perpendicularly ("vertically") to the sample surface, with the C atom bonded to the metallic tip.[2,19,20] We also ignore the vibration of the tip and use an average scanning height ($H_{scan} = z_O - z_{surface}$, being the distance between the O in CO and the sample surface plane, for a planar molecule, or planar part of a molecule, lying parallel to the surface) in our simulations. During the scanning, the metal-CO tip feels the tip-surface interaction force and tilts, as shown in Fig. 1a. The lateral displacement of the O atom $\overrightarrow{\Delta_{lat}}$ depends on the lateral stiffness of the metal-CO tip and the lateral force, which in turn is related to the individual sample molecule and the H_{scan}. For instance, with a Cu3-Cu-CO tip above a pentacene molecule (Fig. 1b) with H_{scan} = 3.4 Å, $\max(|\overrightarrow{\Delta_{lat}}|) \approx 0.2$ Å with $\max(|\overrightarrow{F_{lat}}|) \approx 30$ pN, corresponding to lateral stiffness of 1.5 N/m; the $\max(|\overrightarrow{\Delta_{lat}}|)$ stays close to 0.2 Å for H_{scan} = 4.0 Å, due to the slow decay of the long-range attractive force, while it increases to ~ 0.4 Å for H_{scan} = 2.6 Å. Because of the much longer Cu-C-O distance (~ 2.95 Å), the lateral displacement only yields a small tilt angle θ ~ 0 to 10° of the CO at the metallic tip apex, and correspondingly only a very small vertical displacement of the O atom (Δz ~ 0.03 Å for a 0.4 Å lateral displacement). In addition, for typical parameters of the cantilever, the vertical tip-surface interaction force (usually less than 100 pN) is much weaker than the axial strength of the C-O bond[21] or the metal-C chemical bond,[19] and the stretching frequency of C-O[22] on a metal surface is much larger than the oscillation frequency of the cantilever. Consequently, the vertical metal-C-O length is affected very little by the vertical interaction force. To confirm this, relaxing a metal-C-O tip over a sample molecule where the vertical interaction force is 80 pN and the lateral force is zero due to symmetry gives a vertical

displacement of the O atom of ~ 0.002 Å. Therefore, it is a good approximation to omit the vertical displacement of the O atom during the AFM scanning. On the other hand, the lateral displacement of the O atom is much larger and it should be approximately proportional to the lateral interaction force. The corrugation of the lateral force F_x varies very similarly to the lateral oxygen displacement $\overrightarrow{\Delta_{lat}}$ above the molecule area, as shown in Fig. 1c. Outside the area of the sample molecule the short-range interaction (Pauli repulsion) decays fast to zero while the long-range vdW interaction is dominant and acts on the whole tip, resulting in a decreased correlation between the lateral force and displacement. In our model we secondly assume that the lateral displacement of the oxygen atom is linearly proportional to the lateral force when the tilt angle is small, including for the area above the sample molecule that we are most interested in. This assumption has been used by other authors to include the CO tilt effect.[15,23] Thirdly, we assume the interaction force is decisively determined by the position of the oxygen atom relative to the sample, because the Pauli repulsion decays rapidly (exponentially) with increasing tip-surface distance.[13,24]

The above considerations suggest that we must distinguish between, on one hand, the nominal position of the macroscopic tip ($\vec{R}^{tip}$), which is the position that is measured experimentally as if the tip were rigid, and, on the other hand, the actual displaced position of the O of CO ($\vec{R}^{O}$), which is the position that determines the force. At a lateral position $\vec{R}^{tip} = (x, y)$ of the macroscopic tip (taken to be the lateral position of the O atom without tilt), the metal-C-O tip feels the lateral force $\overrightarrow{F_{lat}}$ from the sample surface, tilting the metal-C-O such that the O atom moves to a

new tilted position $\vec{R}^{O} = \left(x_{tilt}, y_{tilt}\right)$. Neglecting the vertical oxygen displacement, the vertical force $F_z^{tilt}(\vec{R}^{tip})$ experienced by the macroscopic tip at its measured nominal position $\vec{R}^{tip} = \left(x, y\right)$ actually corresponds to the vertical force $F_z(\vec{R}^{O})$ experienced by the O atom at its tilt-corrected displaced position $\vec{R}^{O} = \left(x_{tilt}, y_{tilt}\right)$ obtained for the constant height H_{scan}. The lateral displacement of the oxygen atom can be added through $\vec{R}^{O} = \vec{R}^{tip} + \frac{1}{k} \cdot \overrightarrow{F_{lat}}$ assuming a linear relationship between the lateral force and small lateral displacements. The constant k corresponds to the lateral stiffness of the entire metal-C-O tip: when calculated for Cu_2CO, the stiffness k is 0.5 N/m,[5] while experimentally it is measured to be 0.26 N/m.[23] Finally the measured (tilt-corrected) force $F_z^{tilt}(\vec{R}^{tip})$ at the nominal (measured) tip position $\vec{R}^{tip}$ is actually the force $F_z(\vec{R}^{O})$ that acts at the displaced tip position $\vec{R}^{O}$: $F_z^{tilt}(\vec{R}^{tip}) = F_z(\vec{R}^{O})$.

The pair $\left[\vec{R}^{tip}, F_z(\vec{R}^{O})\right]$ corresponds to the experimental data of the measured nominal tip position vs. the vertical force on the bent CO at the tip apex. The AFM image records the tip's frequency shift $\Delta f(x,y,z)$ that can be calculated by differentiating the corresponding $F_z^{tilt}(\vec{R}^{tip})$.[25] The relationship between the frequency shift and the vertical force for small oscillation amplitudes (i.e. ~0.2 Å) of the cantilever is given by Sader and Jarvis[25] which can be simplified as:

$$\Delta f(x,y,z) = -\frac{f_0}{2k_0}\frac{\partial F_z^{tilt}(x,y,z')}{\partial z'}\bigg|_{z'=z} \quad (1)$$

where f_0 and k_0 are the resonance frequency and the spring constant of the macroscopic tip, respectively. Because the tip-surface interaction force is weak (less than 100 pN) during the AFM measurements,[2] very accurate calculations are required. To this end, we used the *Fritz Haber Institute ab initio molecular simulations* (FHI-aims) code package[26] with accurate atomic-centered basis set and grid-based real-space integration of "*tight*" settings, which guarantees an accuracy of the force output within 1 pN. The DFT+vdW method of Tkatchenko and Scheffler (TS)[27] is applied for describing the intermolecular interactions. We chose the generalized gradient approximation of Perdew, Burke, and Ernzerhof (PBE)[28] for the exchange-correlation functional used in the DFT calculations. We first calculated F_z with a rigid tip on a lateral grid of x and y positions with intervals of 0.2 Å. For a flexible tip, the displaced O position $\vec{R}^O$ may well fall in between grid points. In this case, the force $F_z\left(\vec{R}^O\right)$ is estimated by cubic polynomial interpolation. Obviously, in this model three assumptions are used which result in some deviation from the practical AFM images. In details, the simulated maps are less sharp due to the constant height assumption; the non-linear interplay of the Pauli repulsion and the spring force of the tilt of the CO play a role. Nevertheless, as presented in the following, in most cases this model reproduces the AFM images well for discussion.

3. Results and discussion

With this model, we compare an experimental image[2] of pentacene on Cu(111) with the frequency shift image obtained by differentiation of F_z^{tilt} based on eq. (1), as shown in Fig. 2(a,b). The corrected force F_z^{tilt} is calculated with lateral stiffness k = 0.5 N/m for tip heights ranging from H_{scan} = 3.675 Å to 3.75 Å with a vertical spacing of 0.025 Å. The calculations used a pentacene molecule which is first optimized on a Cu(111) surface until the forces are below 1 pN, while the Cu(111) substrate is removed in the subsequent AFM simulations to save calculation cost. The pentacene tilts a little along the long axis.[29] Clearly this pattern shows very good agreement with the experimental results on Cu(111):[2] the C-C bonds are sharp; the two C_6 rings at the two ends are imaged with a more realistic horseshoe shape and the central three C_6 rings are hexagons stretched considerably in the y direction.

It has been observed that the contrast in the vertical force is the same as for the corresponding frequency shift image with a shifted H_{scan} (see the supplementary materials),[2,5,13,17,24] as visually verified by comparison between the frequency shift map in Fig. 2b and the F_z^{tilt} map in Fig. 2c. Consequently, to reduce the calculation cost, in the following our further analysis will be based on direct comparison between F_z^{tilt} and experimental frequency shift images.

An F_z map without lateral effect is shown in Fig. 2d to demonstrate the effect of CO tilt on AFM imaging. The F_z map looks more or less like the experimental image due to the main vertical contribution, but appears much more blurred (see Fig. 1a). The sharper image of Fig. 2c compared to Fig. 2d arises from flexible CO tilt at the tip apex. To demonstrate this point, we scan along the long axis of pentacene on a lateral grid of x positions with a spacing of 0.2 Å. The corresponding forces F_x, F_z and

F_z^{tilt} are shown in Fig. 3a. The lateral force component F_y is close to zero due to symmetry and is thus omitted. The sharper peaks of F_z^{tilt} compared to F_z imply that the CO tilt sharpens the bond images, since the lateral force F_x tilts the CO toward the center of the nearest C_6 ring.[14] This also happens at the two ends of the molecule, but in addition longer range forces like the vdW interaction have the more global effect of tilt the CO molecule toward the molecule center. This leads to a general expansion of bond images (away from the sample molecular center), especially for bonds located further away from the sample molecule center, making the entire molecule look expanded relative to its real size. In our simulation the distance between the first and the sixth C-C bridge bonds is observed to be about 1.0 Å wider than in the actual pentacene, as revealed by the two maxima of the red curve of F_z^{tilt} in Fig. 3a.

The general expansion can be distinguished in the experimental images,[15] while it is more striking that the hexagonal C_6 rings appear stretched considerably in the *y* direction. Visually the α-bond is twice as long as the β-bond in the AFM image, where the α-bond is a C-C bridge bond parallel to the y direction and the β-bond is a C-C bond oriented about $\pm 60^{o}$ from it, as denoted in Fig. 2a. However, the DFT-calculated bond lengths of the central α- and β-bonds in free pentacene are 1.461 and 1.405 Å, respectively, differing only by about 4%;[30] experimental values for these bonds in the pentacene crystal are on average 1.467 and 1.396 Å, respectively, differing by only 5%.[31] We show line profiles along the *y* direction over the ring center and the α-bond of the central C_6 ring in Fig. 3b and 3c. The F_x components along these two lines are zero due to symmetry (see Fig. 3a) and omitted. Compared to F_z (blue curve), F_z^{tilt}

(red curves) including CO tilt exhibits a flattened valley over the ring center (Fig. 3b) and over the α-bond (Fig. 3c), as well as sharper peaks corresponding to C images. Additionally, the maximum repulsive force F_z^{tilt} is located about 0.1 Å of the C1 sites, while it is 0.5 Å outside the C2 site. The two repulsive maxima of F_z^{tilt} along the C-C bridge bond thus lead to peaks outside the C2 sites in the AFM images which could be erroneously assigned to represent the carbon sites. As a result, the apparent α-bond image, which connects the two maxima of F_z^{tilt}, is about 1.0 Å longer than the real bond length, an extension of almost 70%. This large displacement of C2 also considerably modifies the apparent orientation of the β-bond. In contrast, the distance between two C-C bridge bonds changes little (Fig. 3a, red curve) and hence the C_6 rings look much more stretched in the y direction.

It is conjectured that this distortion arises from the lateral effect of CO tilt, but it is difficult to understand why the C_6 rings are much more stretched in the y direction than in the *x* direction.[13-15] For this, we look into the F_z curve (blue) obtained without CO tilt in Fig 3c, of which the F_z maximum, corresponding to the apparent position of C2, is already moving away from the C2 site. The displacement of the F_z maximum from the C2 site is found to depend on H_{scan}, as demonstrated in Fig. 3d: it is located at about 0.1, 0.2, 0.35 and even 0.5 Å outside the C2 position H_{scan} at values of 2.6, 3.0, 3.4 and 3.6 Å. The lateral resolution of F_z disappears with H_{scan} larger than 3.6 Å and the maximum near C2 cannot be located any more. This displacement of F_z maxima from corresponding atom or bond positions is not uniform for different sites of the pentacene. For example, F_z maxima in a range of H_{scan}

(3.0-3.6 Å) shift very little from the C1 site (Fig. 3b) and are displaced by less than 0.2 Å from the first and sixth bonds in pentacene (Fig. 3a). We note that the F_z without any lateral effect is calculated without any assumptions in our simulations. Consequently, it is intrinsic that the chemical structures are distorted in AFM images. This intrinsic effect can be very big, for example, elongation by 30%, 50% and 70% for α-bonds at 3.0, 3.4 and 3.6 Å H_{scan}, respectively.

It has been proposed that contrast of AFM images is related to the electron density distribution of the sample where a greater electron density leads to a stronger repulsive force.[13,24] Although the maxima of total electron density are located at the nuclear positions,[32] the valence electrons of conjugated molecules like pentacene are delocalized π-electrons, and so that the maxima of the valence electron density in overlapping regions can be displaced laterally from the projections of the atom positions. Both the electron density maxima and the force F_z maxima move progressively away from the projected positions of the nuclei, as H_{scan} increases, but the locations of the two kinds of maxima are not the same at a given $H_{scan.}$ We thus conjecture the repulsive force that the tip feels should be considered as an integrated effect arising from the electrons in a region of certain thickness below the tip, for example, dependent on integrated electron density (IED) along the *z* direction from a given height above the sample molecule plane up to the level H_{scan}. The inset in Fig. 3d shows that the IED maximum above the 1.0 Å-height plane is located less than 0.1 Å away from the C2 site, while above the 1.5 and 1.9 Å planed it shifts to about 0.15 and 0.35 Å away from the C2 position, respectively; this explains the H_{scan} dependence of the intrinsic elongation of the α-bond without CO tilt. This is further confirmed with a line profile of the IED above the 1.9 Å plane along the α-bond

(rather than a single point) shown in Fig. 3e which matches well the F_z curve (blue curve in Fig. 3c) obtained at H_{scan}= 3.4 Å, including the positions of F_z maxima and the shape of the valley in between. IED maxima above 2.0 Å become elusive and do not match any atomic positions; we think the IED is too small above 2.0 Å because of the exponential decay of the electron density, which is related to the resolution vanishing in AFM images.

In addition to the intrinsic effect due to displacement of the IED maximum from the atom or bond positions, the extrinsic effect due to CO tilt further distorts the AFM image by shifting positions of F_z maxima. This is determined by the lateral force at the positions of F_z maxima and stiffness of metal-CO tip. In our simulations, the lateral force is found to be around 15 pN at the positions of F_z maxima corresponding to the C-C bridge bonds at the two ends, and around 8 pN at the positions of F_z maxima corresponding to the C1 and C2 sites at H_{scan}=3.4 Å, see Fig. 3a-c. With lateral stiffness k = 0.5 N/m, the outward shift due to CO tilt of the first or sixth bonds is 0.3 Å, adding the intrinsic displacement of 0.2 Å, and thus the total expansion of pentacene along the long axis is 8%; the elongation of the α-bond arises from the intrinsic displacement by 0.35 Å and the extrinsic effect from CO tilt by 0.15 Å, giving an overall elongation of 70%. Consequently, the AFM image of pentacene seems considerably stretched in the y direction. Clearly, a softer tip or larger lateral force will further shift the vertical force maxima, and hence distort the AFM image more. However, the primary feature of the distortion within the pentacene, which is the stretch of the C6 ring in the y direction, is dominated by the intrinsic effect, while the extrinsic effect due to CO tilt is more or less a general expansion distortion.

The extension of the α-bond in experiments is approximately 70%, 40% and 100% for pentacene on Cu(111)[2], Cu(111)[15] and NaCl/Cu(111) substrates[15], respectively. In our simulations, 30 – 70% elongation of the α-bond could arise from the intrinsic effect dependent on H_{scan}. It is noted that in our simulations the substrate effect is ignored to save calculation cost. By including different lateral forces from the substrate,[15] the dramatic distortions in experiments can be understood for a reasonable lateral stiffness of the tip.

Another example to demonstrate dramatic distortion in AFM image is the adsorption of C_{60} on Cu(111) exposing a near-hexagonal C_6 face. The C-C bond joining two hexagons (h-bond) is has an apparent length that is 30% shorter than that joining a pentagon and a hexagon (p-bond) in AFM images,[5] although in the chemical structure these bond lengths only differ by about 4%.[33] We show in Fig. 4b that the F_z^{tilt} pattern is in close agreement with the experimental image obtained at z = 3.6 Å;[5] the bright ring corresponds to the exposed C_6 ring. By locating positions of the maximum repulsive forces on the F_z^{tilt} map, it is easy to find the apparent location of the C-C bonds: the h-bond and the p-bond are shifted by about 0.37 and 0.27 Å, respectively, away from the molecular center; The resulting apparent lengths of the h- and p-bonds are 1.6 and 2.3 Å, respectively, differing by about 25%, as denoted by dashed yellow lines in the F_z^{tilt} pattern.

The bond length difference is due to the fact that the h-bond is shifted away from the molecular center further than is the p-bond.[5] In our simulations the h-bond is shifted by about 0.1 Å more than the p-bond away from the molecule center, consistent with the result obtained with fully relaxed Cu_2CO tip.[5] It is suggested in our

simulations that outwards shift of the two bonds is an overall result due to the intrinsic and extrinsic effects: F_z maxima are already shifted away from the actual bond locations, 0.17 and 0.08 Å outward from the h- and p-bonds, respectively, while the extrinsic effect due to CO tilt is about 0.2 Å for both bonds, see Fig. 4c. It is important to note that the intrinsic displacement is the cause of the observed displacement by 0.1 Å from an h-bond to a p-bond. This is why our model based on assumptions which could underestimate the tilt effect actually reproduces the shift difference obtained with a fully relaxed Cu_2CO tip.[5] Moreover, the p- and h-bonds are bent in AFM images in addition to the elongated bond lengths, as shown in Fig. 4b or in experiments.[5] The distortion of the bent bonds can only be understood with the intrinsic effect. A 2-dimensional IED contour above 1.8 Å from C_6 plane to H_{scan} is shown in Fig. 4d to compare with a hexagon therein indicating the C_6 positions: the maxima of the IED outside the middle points of the h- and p-bond explain the intrinsic outwards shift, and connection of the IED maxima near the C_6 hexagon reveals the intrinsic distortion of the bond shapes, bent C-C bonds rather than straight ones.

Based on the above discussion, the intrinsic effect is the primary effect in the distorted AFM images and dominates the main features of the distorted structures, although the atomic positions could be displaced even more by the extrinsic effect due to CO tilt. The intrinsic distortion could be crucial to interpret the distorted images. For example, according to the intrinsic distortion within pentacene and C_{60}, we find that the vertical force F_z maximum near the C1 site in pentacene or near the p-bond in C_{60} will only shift a little in a reasonable range of H_{scan}. This means that some sites in AFM images can be used as references and are assumed displaced fully due to CO tilt. By this approach, the extrinsic distortion by CO tilt could be excluded,[15] and then

details of the image with intrinsic distortion can be understood by comparing it with the theoretical results. This will be explored in future work.

4. Conclusion

In summary, our model based on a detailed *ab initio* calculation of the tip-surface interaction for flexible CO-functionalized tips can generate patterns which agree very well with experimental images. A big advantage of our model is that it is a process comprised of two steps: firstly the F_z can be calculated without assumptions and the lateral effect is introduced afterwards with artificial lateral stiffness of the CO at the metallic tip apex. In this way intrinsic and lateral effects can be decomposed and studied separately. With direct comparison between simulated two-dimensional maps and experimental images, we confirm that the CO tilt indeed sharpens the bonds and artificially expands the AFM images. We further found that distortion in AFM images is mainly determined by an intrinsic effect originating from the integrated electron density in the tip-sample overlap region moving away from (the vertical projection of) the atom or bond positions. This intrinsic effect is of crucial importance to understand or interpret the distorted AFM images.

Acknowledgments

We thank Z.H. Cheng for fruitful discussions. This work was supported by the Natural Science Foundation of China (No.51302231, No. 11374276), by the Fundamental Research Funds for the Central Universities (SWJTU2682013RC02, SWJTU11ZT31, 2682013CX004), and in part by project no. 9041650 of the Research

Grants Council of HKSAR. MAVH was supported by the HKBU Strategic Development Fund.

Supporting Information Available: (A high-resolution model for non-contact atomic force microscopy with a flexible molecule on the tip apex) This material is available free of charge via the Internet at http://pubs.acs.org.

References

(1) Albrecht, T. R.; Grutter, P.; Horne, D.; Rugar, D. Frequency-Modulation Detection Using High-Q Cantilevers for Enhanced Force Microscope Sensitivity. *J. Appl. Phys.* **1991**, *69*, 668-673.

(2) Gross, L.; Mohn, F.; Moll, N.; Liljeroth, P.; Meyer, G. The Chemical Structure of a Molecule Resolved by Atomic Force Microscopy. *Science* **2009**, *325*, 1110-1114.

(3) Gross, L.; Mohn, F.; Moll, N.; Meyer, G.; Ebel, R.; Abdel-Mageed, W. M.; Jaspars, M. Organic Structure Determination Using Atomic-Resolution Scanning Probe Microscopy. *Nature Chemistry* **2010**, *2*, 821-825.

(4) Boneschanscher, M. P.; van der Lit, J.; Sun, Z.; Swart, I.; Liljeroth, P.; Vanmaekelbergh, D. Quantitative Atomic Resolution Force Imaging on Epitaxial Graphene with Reactive and Nonreactive Afm Probes. *ACS Nano* **2012**, *6*, 10216-10221.

(5) Gross, L.; Mohn, F.; Moll, N.; Schuler, B.; Criado, A.; Guitian, E.; Pena, D.; Gourdon, A.; Meyer, G. Bond-Order Discrimination by Atomic Force Microscopy. *Science* **2012**, *337*, 1326-1329.

(6) de Oteyza, D. G.; Gorman, P.; Chen, Y.-C.; Wickenburg, S.; Riss, A.; Mowbray, D. J.; Etkin, G.; Pedramrazi, Z.; Tsai, H.-Z.; Rubio, A.; Crommie, M. F.; Fischer, F. R. Direct Imaging of Covalent Bond Structure in Single-Molecule Chemical Reactions. *Science* **2013**, *340*, 1434-1437.

(7) Schuler, B.; Liu, W.; Tkatchenko, A.; Moll, N.; Meyer, G.; Mistry, A.; Fox, D.; Gross, L. Adsorption Geometry Determination of Single Molecules by Atomic Force Microscopy. *Phys. Rev. Lett.* **2013**, *111*, 106103.

(8) Zhang, J.; Chen, P.; Yuan, B.; Ji, W.; Cheng, Z.; Qiu, X. Real-Space Identification of Intermolecular Bonding with Atomic Force Microscopy. *Science* **2013**, *342*, 611-614.

(9) van der Lit, J.; Boneschanscher, M. P.; Vanmaekelbergh, D.; Ijas, M.; Uppstu, A.; Ervasti, M.; Harju, A.; Liljeroth, P.; Swart, I. Suppression of Electron-Vibron Coupling in Graphene Nanoribbons Contacted Via a Single Atom. *Nature Communications* **2013**, *4*, 2023.

(10) Albrecht, F.; Neu, M.; Quest, C.; Swart, I.; Repp, J. Formation and Characterization of a Molecule-Metal-Molecule Bridge in Real Space. *J. Am. Chem. Soc.* **2013**, *135*, 9200-9203.

(11) Welker, J.; Weymouth, A. J.; Giessibl, F. J. The Influence of Chemical Bonding Configuration on Atomic Identification by Force Spectroscopy. *ACS Nano* **2013**, *7*, 7377-7382.

(12) Welker, J.; Giessibl, F. J. Revealing the Angular Symmetry of Chemical Bonds by Atomic Force Microscopy. *Science* **2012**, *336*, 444-449.

(13) Moll, N.; Gross, L.; Mohn, F.; Curioni, A.; Meyer, G. The Mechanisms Underlying the Enhanced Resolution of Atomic Force Microscopy with Functionalized Tips. *New Journal of Physics*

2010, *12*, 125020.

(14) Boneschanscher, M. P.; Hamalainen, S. K.; Liljeroth, P.; Swart, I. Sample Corrugation Affects the Apparent Bond Lengths in Atomic Force Microscopy. *ACS Nano* **2014**, *8*, 3006-3014.

(15) Neu, M.; Moll, N.; Gross, L.; Meyer, G.; Giessibl, F. J.; Repp, J. Image Correction for Atomic Force Microscopy Images with Functionalized Tips. *Phys. Rev. B* **2014**, *89*, 205407.

(16) Moll, N.; Schuler, B.; Kawai, S.; Xu, F.; Lifen Peng, L.; Orita, A.; Otera, J.; Curioni, Alessandro.; Neu, M.; Repp, J.; Meyer, G.; Gross, L; Image Distortions of a Partially Fluorinated Hydrocarbon Molecule in Atomic Force Microscopy with Carbon Monoxide Terminated Tips. dx.doi.org/10.1021/nl502113z

(17) Guo, C. S.; Van Hove, M. A.; Zhang, R. Q.; Minot, C. Prospects for Resolving Chemical Structure by Atomic Force Microscopy: A First-Principles Study. *Langmuir* **2010**, *26*, 16271-16277.

(18) Hapala, P.; Kichin, G.; Wagner, C.; Tautz, F. S.; Temirov, R.; Jelínek, P. Mechanism of High-Resolution Stm/Afm Imaging with Functionalized Tips. *Phys. Rev. B* **2014**, *90*, 085421.

(19) Schimka, L.; Harl, J.; Stroppa, A.; Grueneis, A.; Marsman, M.; Mittendorfer, F.; Kresse, G. Accurate Surface and Adsorption Energies from Many-Body Perturbation Theory. *Nat. Mater.* **2010**, *9*, 741-744.

(20) Ren, X.; Rinke, P.; Scheffler, M. Exploring the Random Phase Approximation: Application to Co Adsorbed on Cu(111). *Phys. Rev. B* **2009**, *80*, 045402.

(21) Common Bond Energies (D) and Bond Lengths (r), wiredchemist.com

(22) Persson, B. N. J.; Ryberg, R. Collective Vibrational Modes in Isotopic Mixtures of Co Adsorbed on Cu(100). *Solid State Commun.* **1980**, *36*, 613-617.

(23) Weymouth, A. J.; Hofmann, T.; Giessibl, F. J. Quantifying Molecular Stiffness and Interaction with Lateral Force Microscopy. *Science* **2014**, *343*, 1120-1122.

(24) Moll, N.; Gross, L.; Mohn, F.; Curioni, A.; Meyer, G. A Simple Model of Molecular Imaging with Noncontact Atomic Force Microscopy. *New Journal of Physics* **2012**, *14*, 083023.

(25) Sader, J. E.; Jarvis, S. P. Accurate Formulas for Interaction Force and Energy in Frequency Modulation Force Spectroscopy. *Appl. Phys. Lett.* **2004**, *84*, 1801-1803.

(26) Blum, V.; Gehrke, R.; Hanke, F.; Havu, P.; Havu, V.; Ren, X.; Reuter, K.; Scheffler, M. Ab Initio Molecular Simulations with Numeric Atom-Centered Orbitals. *Computer Physics Communications* **2009**, *180*, 2175-2196.

(27) Tkatchenko, A.; Scheffler, M. Accurate Molecular Van Der Waals Interactions from Ground-State Electron Density and Free-Atom Reference Data. *Phys. Rev. Lett.* **2009**, *102*, 073005.

(28) Perdew, J. P.; Burke, K.; Ernzerhof, M. Generalized Gradient Approximation Made Simple. *Phys. Rev. Lett.* **1996**, *77*, 3865-3868.

(29) Shi, X. Q.; Li, Y.; Van Hove, M. A.; Zhang, R. Q. Interactions between Organics and Metal Surfaces in the Intermediate Regime between Physisorption and Chemisorption. *Journal of Physical Chemistry C* **2012**, *116*, 23603-23607.

(30) Endres, R. G.; Fong, C. Y.; Yang, L. H.; Witte, G.; Woll, C. Structural and Electronic Properties of Pentacene Molecule and Molecular Pentacene Solid. *Comp. Mater. Sci.* **2004**, *29*, 362-370.

(31) Campbell, R. B.; Monteath Robertson, J.;Trotter, J. Acta Cryst. 14, 705 (1961)

(32) Cherif F. Matta and Russell J. Boyd, The quantum theory of atoms in molecules,WILEY-VCH 2007.

(33) Dresselhaus, M. S.; Dresselhaus, G.; Eklund, P. C. Science of Fullerenes and Carbon Nanotubes, Academic Press, California 1996.

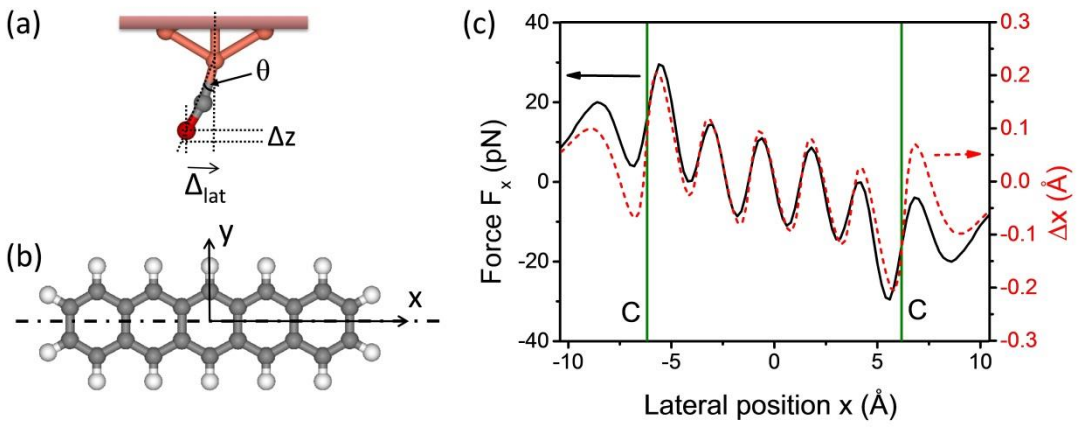

Fig. 1. (a) Schematic diagram of the lateral tilt of CO at a metallic Cu tip apex during AFM scanning. Cu atoms are shown in orange, C in gray and O in red. The tilt angle is exaggerated for clarity. (b) The chemical structure of a pentacene molecule; the dashed-dotted line denotes the long axis along which scanning with a Cu_3-Cu-C-O tip produces the lateral force and oxygen displacement of panel (c). (c) The black curve shows the lateral force in the *x* direction while the red dashed curve denotes the lateral displacement of O atom (all Cu atoms are constrained). The lateral displacement is defined as $\Delta x = x_O - x_{Cu}$. The two green vertical lines denote the positions of the first and sixth C-C bridge bonds.

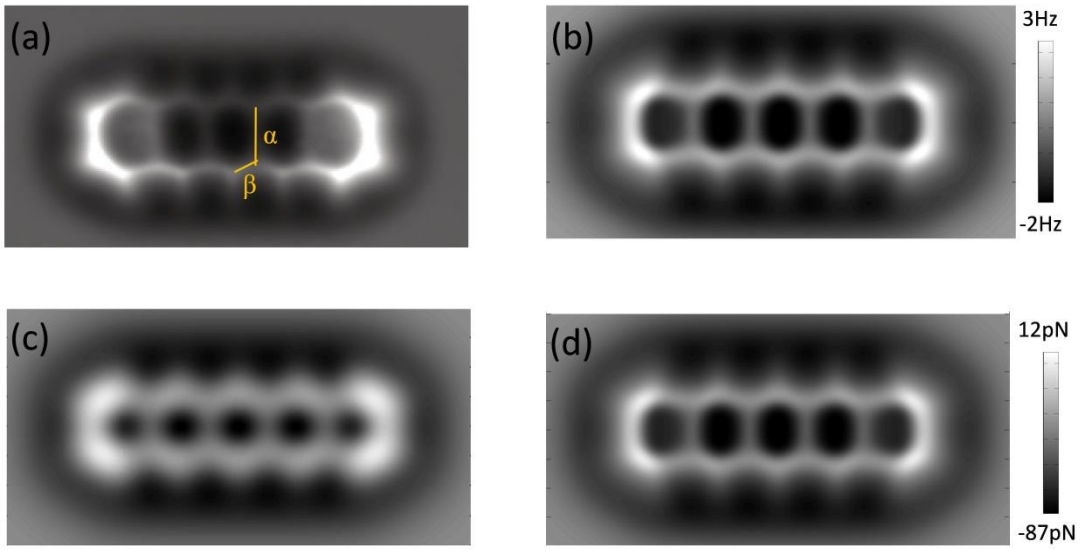

Fig. 2 (a) Experimental AFM image of pentacene on Cu(111).[2] The α-bond is a C-C bridge bond and the β-bond is a C-C bond connected to it; (b) frequency shift image at H_{scan} = 3.7 Å based on F_z^{tilt}. (c) F_z^{tilt} map and (d) F_z map without lateral effect at H_{scan} = 3.4 Å. F_z^{tilt} is obtained with lateral stiffness k = 0.5 N/m.

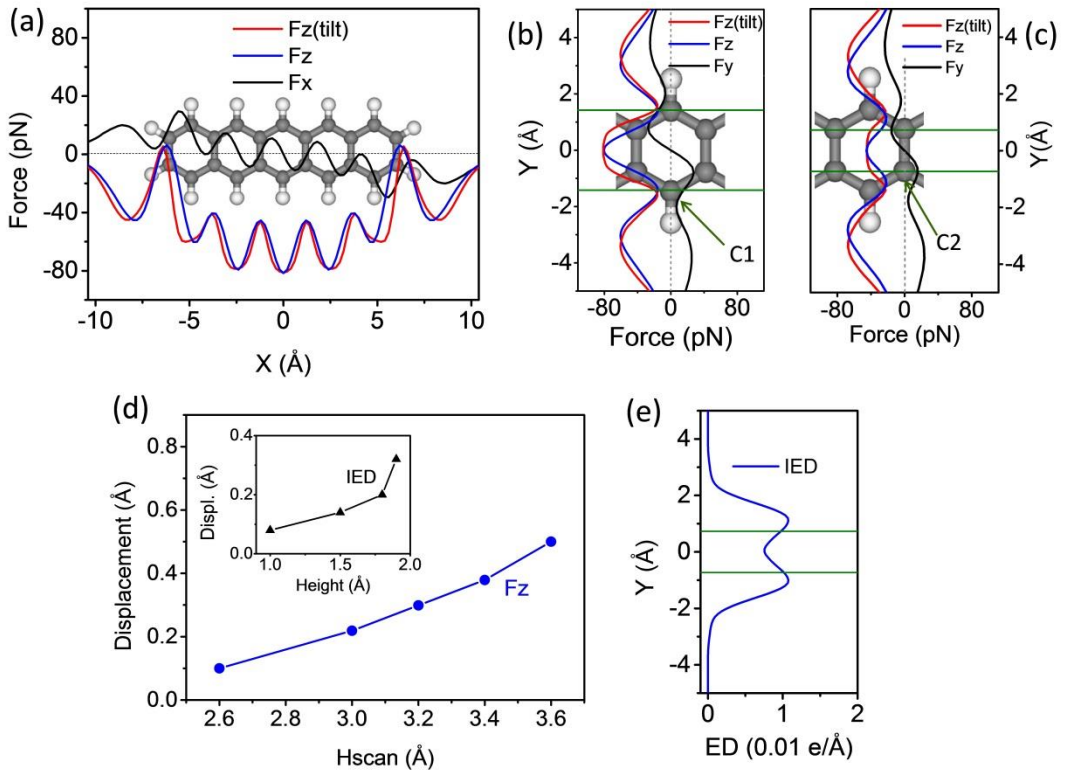

Fig. 3. (a), (b) and (c) Scans (along the dotted black lines) of F_x, F_y, F_z and F_z^{tilt} shown as black, black, blue and red curves. C1, and C2 sites are denoted by arrows. The maps and line profiles are obtained at H_{scan} = 3.4 Å and F_z^{tilt} obtained with k = 0.5 N/m; (d) Displacement from C2 site along the α-bond of the F_z maximum and (insect) integrated electron density ranging from different planes above the molecule to H_{scan} (see the text); (e) Line profile of integrated electron density above 1.9 Å along the α-bond. The green lines mark the positions of C.

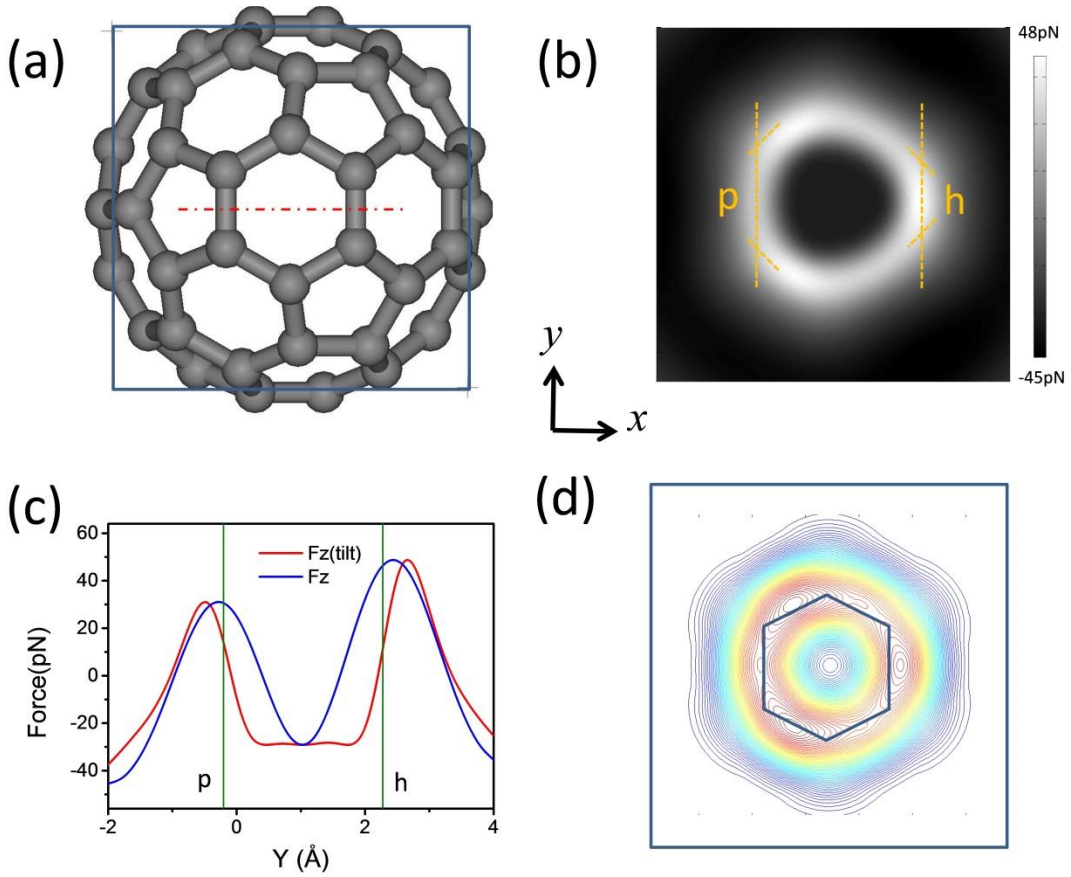

Fig. 4 (a) Atomic structure of C_{60}, (b) simulated F_z^{tilt} pattern with a size 6.8 by 6.8 Å^2 (c). Line profile of F_z and F_z^{tilt} along the red dash-dotted line in the chemical structure figure, and (d) Integrated electron density contours (red/blue=high/low density) ranging from 1.8 Å above C_6 plane to H_{scan}, where the hexagon denotes the C_6 positions. The blue box denotes the scanned area. The maps and line profiles are obtained at H_{scan} = 3.3 Å and F_z^{tilt} obtained with k = 0.5 N/m.

TOC